J|A|C|S
ARTICLES

Conformation-Dependent Ligand Regulation of ATP Hydrolysis by Human KSP: Activation of Basal Hydrolysis and Inhibition of Microtubule-Stimulated Hydrolysis by a Single, Small Molecule Modulator

Lusong Luo,*,† Jeffrey D. Carson,† Kathleen S. Molnar,‖ Steven J. Tuske,‖ Stephen J. Coales,‖ Yoshitomo Hamuro,‖ Chiu-mei Sung,§ Valery Sudakin,§ Kurt R. Auger,§ Dashyant Dhanak,‡ Jeffrey R. Jackson,§ Pearl S. Huang,§ Peter J. Tummino,† and Robert A. Copeland*,†

Department of Enzymology and Mechanistic Pharmacology, Oncology CEDD, Department of Medicinal Chemistry, Oncology CEDD, and Department of Oncology Biology, Oncology CEDD, GlaxoSmithKline, Collegeville, Pennsylvania 19426, and ExSAR Corporation, 11 Deer Park Drive, Suite 103, Monmouth Junction, New Jersey 08852

Received December 6, 2007; E-mail: lusong.luo@gsk.com; robert.a.copeland@gsk.com

Abstract: Human kinesin spindle protein (KSP)/hsEg5, a member of the kinesin-5 family, is essential for mitotic spindle assembly in dividing human cells and is required for cell cycle progression through mitosis. Inhibition of the ATPase activity of KSP leads to cell cycle arrest during mitosis and subsequent cell death. Ispinesib (SB-715992), a potent and selective inhibitor of KSP, is currently in phase II clinical trials for the treatment of multiple tumor types. Mutations that attenuate Ispinesib binding to KSP in vitro have been identified, highlighting the need for inhibitors that target different binding sites and inhibit KSP activity by novel mechanisms. We report here a small-molecule modulator, KSPA-1, that activates KSP-catalyzed ATP hydrolysis in the absence of microtubules yet inhibits microtubule-stimulated ATP hydrolysis by KSP. KSPA-1 inhibits cell proliferation and induces monopolar-spindle formation in tumor cells. Results from kinetic analyses, microtubule (MT) binding competition assays, and hydrogen/deuterium-exchange studies show that KSPA-1 does not compete directly for microtubule binding. Rather, this compound acts by driving a conformational change in the KSP motor domain and disrupts productive ATP turnover stimulated by MT. These findings provide a novel mechanism for targeting KSP and perhaps other mitotic kinesins.

Introduction

The mitotic spindle has been identified as an important target in cancer chemotherapy because of its critical role in cell division. Microtubule-targeting drugs such as taxanes and vinca alkaloids inhibit the mitotic spindle assembly by disruption of microtubule dynamics. Despite the success of these classes of drugs in the clinic, their clinical applications are limited both by the development of resistance and by significant toxicities. Inhibition of mitotic kinesins represents a promising alternative strategy for antimitotic therapy.[1–5] Mitotic kinesins are ATP-driven motor proteins that play critical roles in the transport of cellular organelles and vesicles and in spindle pole separation and chromosome movement.[6,7] Kinesin spindle protein (KSP or hsEg5) is a particularly attractive antimitotic target in the mitotic kinesin family. KSP generates the major plus-end directed force for mitotic spindle assembly and is essential for spindle pole separation during mitosis. A number of inhibitors of KSP have been reported, including quinazolinone analogues [*Ispinesib* (SB715992), and SB-743921], monastrol, *S*-trityl-L-cysteine, and dihydropyrazoles.[5,8–14] All of these reported inhibitors are suggested to bind to an allosteric binding pocket formed by helices α2 and α3 and loop L5 of the protein. Recent studies have shown that mutations in this binding pocket can generate inhibitor-resistant, but otherwise catalytically competent KSP motor protein.[12,15,16] In particular, *Ispinesib*-resistant KSP mutants D130V and A133D were generated in HCT116 colorectal tumor cells in the presence of *Ispinesib* analogues.[12] Both mutations are located in the loop L5 binding pocket, highlighting a potential mechanism of drug resistance for loop L5 binding inhibitors of KSP. In this study, we report the

† Department of Enzymology and Mechanistic Pharmacology, GlaxoSmithKline.
‖ ExSAR Corporation.
§ Department of Oncology Biology, GlaxoSmithKline.
‡ Department of Medicinal Chemistry, GlaxoSmithKline.

(1) Bergnes, G.; Brejc, K.; Belmont, L. *Curr. Top. Med. Chem.* **2005**, *5*, 127–145.
(2) Duhl, D. M.; Renhowe, P. A. *Curr. Opin. Drug Discovery Dev.* **2005**, *8*, 431–436.
(3) Jackson, J. R.; Patrick, D. R.; Dar, M. M.; Huang, P. S. *Nat. Rev. Cancer* **2007**, *7*, 107–117.
(4) Miglarese, M. R.; Carlson, R. O. *Expert. Opin. Investig. Drugs* **2006**, *15*, 1411–1425.
(5) Sakowicz, R.; Finer, J. T.; Beraud, C.; Crompton, A.; Lewis, E.; Fritsch, A.; Lee, Y.; Mak, J.; Moody, R.; Turincio, R.; Chabala, J. C.; Gonzales, P.; Roth, S.; Weitman, S.; Wood, K. W. *Cancer Res.* **2004**, *64*, 3276–3280.
(6) Miki, H.; Okada, Y.; Hirokawa, N. *Trends Cell Biol.* **2005**, *15*, 467–476.
(7) Kinbara, K.; Aida, T. *Chem. Rev.* **2005**, *105*, 1377–1400.

10.1021/ja710889h CCC: $40.75
Published on Web 05/21/2008

characterization of a novel small molecule modulator of KSP. This compound, KSPA-1, has drastically different effects on KSP ATPase activity in the presence and absence of microtubules (MT). It increases the rate of ATP turnover by the KSP motor domain without MT and conversely blocks the MT-stimulated ATP turnover by KSP. KSPA-1 inhibits the proliferation of tumor cells and induces monopolar spindle formation, which is the same phenotype observed for tumor cells treated with allosteric inhibitors such as *Ispinesib* and monastrol. Kinetic analyses and hydrogen/deuterium-exchange studies suggest that this compound inhibits the microtubule stimulated ATPase activity of KSP by driving conformational changes in the KSP motor domain and disrupting MT-stimulated productive ATP turnover.

Materials and Methods

Materials. Pyruvate kinase/lactate dehydrogenase enzymes were purchased from Sigma. The motor domain of wild-type KSP monomer (amino acids 1−360) was expressed in *Escherichia coli* BL21(DE3) as a C-terminal 6-his fusion protein following procedures previously described.[5,17] Bacterial pellets were lysed with a microfluidizer (Microfluidics Corp.) in lysis buffer [50 mM Tris-HCl, 50 mM KCl, 10 mM imidazole, 2 mM $MgCl_2$, 8 mM β-mercaptoethanol, 0.1 mM ATP (pH 7.4)], and proteins were purified using Ni-NTA agarose affinity chromatography, with an elution buffer consisting of 50 mM PIPES, 10% sucrose, 300 mM imidazole, 50 mM KCl, 2 mM $MgCl_2$, 1 mM β-mercaptoethanol, and 0.1 mM ATP (pH 6.8). KSPA-1 was identified from a high-throughput screen of the GlaxoSmithKline (GSK) compound collection and was synthesized by GSK scientists. Studies on KSPA-1 were performed using solid material (>98% pure). KSPA-1 was soluble up to 250 μM in PEM25 buffer [25 mM PipesK^+(pH 6.8), 2 mM $MgCl_2$, 1 mM EGTA]. The solubility of KSPA-1 was measured using UV−visible absorption spectroscopy. Molecular modeling studies were carried out using MOE (Molecular Operating Environment) (Chemical Computing Group).

Kinetic Characterization of KSP Activation and Inhibition by KSPA-1. Steady-state analyses were carried out using a pyruvate kinase−lactate dehydrogenase detection system that coupled the production of ADP to oxidation of NADH.[17] Absorbance changes were monitored at 340 nm. All biochemical experiments were performed in PEM25 buffer supplemented with 10 μM paclitaxel for experiments involving microtubules. Inhibitor modality under steady-state conditions was determined by measuring the effect of inhibitor concentration on initial velocity as a function of substrate concentration.

Data Analysis. The IC_{50} values and $K_{1/2}$ values reported are mean values ± standard deviation from three independent measurements. IC_{50} values were determined by fitting inhibition data to the binding isotherm (eq 1), where v is the reaction velocity at different concentrations of inhibitor I, v_o is the control velocity in the absence of inhibitor, and n is the Hill Coefficient. $K_{1/2,\text{KSPA-1 activation}}$ values were determined by fitting activation data to the binding isotherm (eq 2), where v is the reaction velocity at different concentrations of activator L, v_o is the control velocity in the absence of activator, and n is the Hill Coefficient. Complete inhibition was observed at saturating compound concentration for all IC_{50} determinations.

$$\frac{v}{v_0} = \frac{1}{1+\left(\frac{[\mathrm{I}]}{\mathrm{IC}_{50}}\right)^n} \tag{1}$$

$$\frac{v}{v_0} = \frac{1}{1+\left(\frac{[\mathrm{L}]}{K_{1/2,\text{activation}}}\right)^n} \tag{2}$$

Mode of inhibition data were fit globally, using the program GraFit, to velocity equations for competitive (eq 3), noncompetitive (eq 4), uncompetitive (eq 6), and mixed inhibition (eq 5). An F test was used to compare the goodness of the fits.

$$\text{competitive inhibition:}\quad v = \frac{V_{\max}S}{K_{\mathrm{m}}\left(1+\frac{I}{K_i}\right)+S} \tag{3}$$

$$\text{noncompetitive inhibition:}\quad v = \frac{V_{\max}S}{K_{\mathrm{m}}\left(1+\frac{I}{K_i}\right)+S\left(1+\frac{I}{K_i}\right)} \tag{4}$$

$$\text{mixed inhibition:}\quad v = \frac{V_{\max}S}{K_{\mathrm{m}}\left(1+\frac{I}{K_i}\right)+S\left(1+\frac{I}{K_i'}\right)} \tag{5}$$

$$\text{uncompetitive inhibition:}\quad v = \frac{V_{\max}S}{K_m+S\left(1+\frac{I}{K_i}\right)} \tag{6}$$

Mant-ADP Release Assay. To monitor 2′-/3′- *O*- (*N*′-methylanthraniloyl)−ADP (Mant-ADP) release, KSP protein was incubated with an excess of Mant-ADP for 30 min at room temperature. Unbound ADP was separated from the KSP protein by gel filtration on a DG10 prepacked column (BioRad), equilibrated with PEM25 buffer. This KSP-Mant-ADP complex was diluted to 5 μM in PEM25 with KSPA-1or DMSO and rapidly mixed in a stopped-flow apparatus with an equal volume of 2 mM ATP solution in PEM25 (with or without 20 μM taxol-polymerized tubulin). Release of Mant-ADP from KSP was monitored by fluorescence (excitation wavelength, 360 nm; emission wavelength, 420 nm) versus time. Resulting fluorescence change traces were fitted with exponential decay curves to determine corresponding rate constants.

MT Binding Competition Assay. Five μM KSP and 5 μM MT were incubated with 0−80 μM KSPA-1 for 30 min at room temperature. These reactions were then subjected to ultracentrifugation for 45 min at 100000*g*. The supernatants and pellets were separated and subjected to electrophoresis on a 4−12% Bis-Tris SDS gel.

Proliferation Assays. Cells were plated in duplicate or triplicate 96-well plates (500 cells/well) and incubated overnight in growth medium. Test compounds in DMSO stocks were serially diluted in DMSO, diluted into growth medium, and then stamped into 96-

(8) Cox, C. D.; Torrent, M.; Breslin, M. J.; Mariano, B. J.; Whitman, D. B.; Coleman, P. J.; Buser, C. A.; Walsh, E. S.; Hamilton, K.; Schaber, M. D.; Lobell, R. B.; Tao, W.; South, V. J.; Kohl, N. E.; Yan, Y.; Kuo, L. C.; Prueksaritanont, T.; Slaughter, D. E.; Li, C.; Mahan, E.; Lu, B.; Hartman, G. D. *Bioorg. Med. Chem. Lett.* **2006**, *16*, 3175–3179.
(9) Skoufias, D. A.; DeBonis, S.; Saoudi, Y.; Lebeau, L.; Crevel, I.; Cross, R.; Wade, R. H.; Hackney, D.; Kozielski, F. *J. Biol. Chem.* **2006**, *281*, 17559–17569.
(10) Cochran, J. C.; Gatial, J. E.; Kapoor, T. M.; Gilbert, S. P. *J. Biol. Chem.* **2005**, *280*, 12658–12667.
(11) Maliga, Z.; Kapoor, T. M.; Mitchison, T. J. *Chem. Biol.* **2002**, *9*, 989–996.
(12) Jackson, J. R.; Auger, K. R.; Gilmartin, A.; Eng, W. K.; Luo, L.; Concha, N.; Parrish, C.; Sutton, D.; Diamond, M.; Giardiniere, M.; Zhang, S.-Y.; Huang, P.; Wood, K. W.; Belmont, L.; Lee, Y.; Bergnes, G.; Anderson, R.; Brejc, K.; Sakowicz, R. *A Resistance Mechanism for the KSP Inhibitor Ispinesib Implicates Point Mutations in the Compound Binding Site*; Presented at the 17th AACR-NCI-EORTC International Conference on Molecular Targets and Cancer Therapeutics, Philadelphia, PA, Nov, 2005; Poster C207.
(13) Cox, C. D.; Breslin, M. J.; Mariano, B. J.; Coleman, P. J.; Buser, C. A.; Walsh, E. S.; Hamilton, K.; Huber, H. E.; Kohl, N. E.; Torrent, M.; Yan, Y.; Kuo, L. C.; Hartman, G. D. *Bioorg. Med. Chem. Lett.* **2005**, *15*, 2041–2045.
(14) Sarli, V.; Giannis, A. *ChemMedChem.* **2006**, *1*, 293–298.
(15) Brier, S.; Lemaire, D.; DeBonis, S.; Forest, E.; Kozielski, F. *J. Mol. Biol.* **2006**, *360*, 360–376.
(16) Maliga, Z.; Mitchison, T. J. *BMC. Chem. Biol.* **2006**, *6*, 2.
(17) Luo, L.; Carson, J. D.; Dhanak, D.; Jackson, J. R.; Huang, P. S.; Lee, Y.; Sakowicz, R.; Copeland, R. A. *Biochemistry* **2004**, *43*, 15258–15266.

well plates containing cells. All plates included a DMSO control and wells with no cells were used to subtract nonspecific background. A cell plate that was not exposed to compound was harvested at the time of compound addition to serve as the time zero ($t = 0$) control. After cells were incubated with compound for 72 h, plates were harvested and the cellular response was determined with CTG (Cell Titer Glo, Promega). The extent of cell proliferation was expressed as a function of cell growth for the DMSO controls and concentration−response curves were fit using XLFit (v4.2) in Microsoft Excel.

Hydrogen/Deuterium-Exchange (H/D-Ex) Analysis. The exchange reaction was initiated by mixing KSP solution (with and without apyrase treatment, and with and without 600 μM KSPA-1) and PEM25 buffer with or without 600 μM KSPA-1 in D_2O. In the exchange solution, the final concentrations were: [KSP] = 17 μM, [KSPA-1] = ±600 μM, [ADP] = ±500 μM, [DMSO] = 6%, and [D_2O] = 80%. The reaction mixture was incubated at 4 ± 1 °C for varying incubation times (15, 50, 150, 500, and 1500 s). These functionally deuterated samples were then subjected to H/D-Ex analysis along with control samples of nondeuterated and fully deuterated protein (incubated in 100 mM TCEP in 80% D_2O at 60 °C overnight). The detailed general operation procedures for H/D-Ex are as described previously.[18] Briefly, a 20 μL H/D-exchanged protein solution was quenched by shifting to pH 2.5, 0 °C with 30 μL of 2 M urea and 1 M TCEP.The quenched solution was immediately passed over an immobilized pepsin column (104 μL bed volume) at 1 °C with 0.05% TFA (200 μL/min) for 3 min with contemporaneous collection of proteolytic products by a trap column. Subsequently the peptide fragments were eluted from the trap column and separated by C18 column (Magic C18, Michrom BioResources, Inc., Auburn, CA) with a linear gradient of 13% to 40% B over 23 min (solvent A, 0.05% TFA in water; solvent B, 95% acetonitrile, 5% water, 0.0025% TFA; flow rate 5−10 μL/min). MS analyses were carried out with a Thermo Finnigan LCQ mass spectrometer (Thermo Electron Corporation, San Jose, CA) with capillary temperature at 215 °C. The centroids of probe peptide isotopic envelopes were measured using an in-house-developed program in collaboration with Sierra Analytics. The corrections for back-exchange were made employing methods described previously.[19,20]

$$\text{deuteration level } (\%) = \frac{m(P) - m(N)}{m(F) - m(N)} \times 100 \qquad (7)$$

where m(P), m(N), and m(F) are the centroid value of partially deuterated peptide, nondeuterated peptide, and fully deuterated peptide, respectively.

Results

Identification of KSP Basal ATPase Activators. The identification of KSP mutations at the *Ispinesib* binding site that could result in drug resistance led us to screen chemical libraries for new inhibitors of KSP with distinct binding sites and enzymatic modes of inhibition. One compound series, the maleamide compounds, was identified from a high-through screen of the GSK compound collection. The maleamide compounds were found to activate ATP turnover by KSP in the absence of MT and inhibit KSP ATP turnover in the presence of MT. One representative compound, KSP activator-1 (KSPA-1, Figure 1a), accelerates the basal ATP turnover rate circa 10-fold from 0.13 to 1.2 s^{-1} at 50 μM. The activation is compound-concentration dependent and saturable (Figure 1b); for KSPA-1 with half-maximal activation ($K_{1/2,\text{KSPA-1 activation}}$) equal to 6.9 ± 0.7 μM. Interestingly, the activation of basal ATP turnover was found to be motor domain specific. No activation was observed for

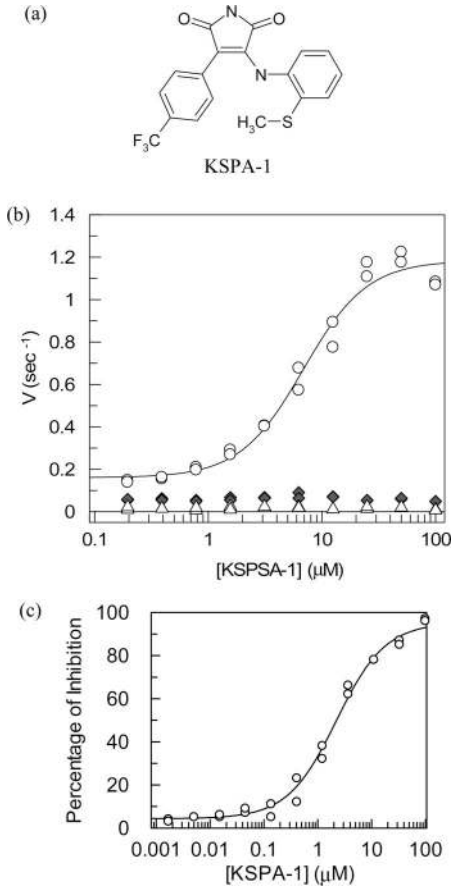

Figure 1. Activation of the basal ATPase activity of kinesins by the maleamide compound KSPA-1: (a) Chemical structure of KSPA-1. (b) Increase of basal kinesin ATPase activity by maleamide compound KSPA-1. The reactions contain 500 nM KSP (open circle), CENP-E (filled diamond), or Kif15 (open triangle). The $K_{1/2,\text{KSPA-1 activation}}$ value was determined by fitting the activity data to eq 2. (c) Representative titration curve of KSPA-1 concentration vs inhibition of KSP-catalyzed ATP hydrolysis (50 nM KSP at saturating MT). The IC_{50} value was determined by fitting inhibition data to the standard binding isotherm (eq 1).

Table 1. Steady-State Kinetic Parameters for KSP Activities in the Presence and Absence of KSPA-1

	MT-free KSP	MT-free KSP + 50 μM KSPA-1	KSP + MT	KSP + MT + 30 μM KSPA-1
k_{cat} (s^{-1})	0.20 ± 0.01	1.4 ± 0.1	13 ± 1	4.4 ± 0.1
$K_{m_{[ATP]}}$ (μM)	30 ± 4	46 ± 5	14 ± 1	103 ± 14
$k_{cat}/K_{m_{[ATP]}}$ (s^{-1} M^{-1})	6.7×10^3	3.0×10^4	9.3×10^5	4.3×10^4
$K_{1/2,MT}$ (μM)	NA	NA	0.27 ± 0.01	0.31 ± 0.01
$K_{1/2,\text{KSPA-1 activation}}$ (μM)	6.9 ± 0.7	NA	NA	NA

CENP-E or Kif15 catalyzed basal ATP turnover (Figure 1b). In the presence of MT, KSPA-1 inhibits KSP activity with an IC_{50} = 2.3 ± 0.3 μM (see Figure 1c for a representative titration curve). No inhibition of other kinesins, including CENP-E and Kif15 was observed. In addition, dilution experiments showed that the activation and inhibition effects of KSPA-1 are rapidly reversible (data not shown), which excludes the possibility of covalent modification of KSP by KSPA-1.

Biochemical Mechanism of Action of Maleamide KSP Activators. To understand the biochemical mechanism of basal KSP activation, we examined the effects of KSPA-1 on both the k_{cat} and K_m for KSP-catalyzed basal ATP hydrolysis reaction.

(18) Hamuro, Y.; Coales, S. J.; Southern, M. R.; Nemeth-Cawley, J. F.; Stranz, D. D.; Griffin, P. R. *J. Biomol. Tech.* **2003**, *14*, 171–182.
(19) Bai, Y.; Milne, J. S.; Mayne, L.; Englander, S. W. *Proteins* **1993**, *17*, 75–86.
(20) Zhang, Z.; Smith, D. L. *Protein Sci.* **1993**, *2*, 522–531.

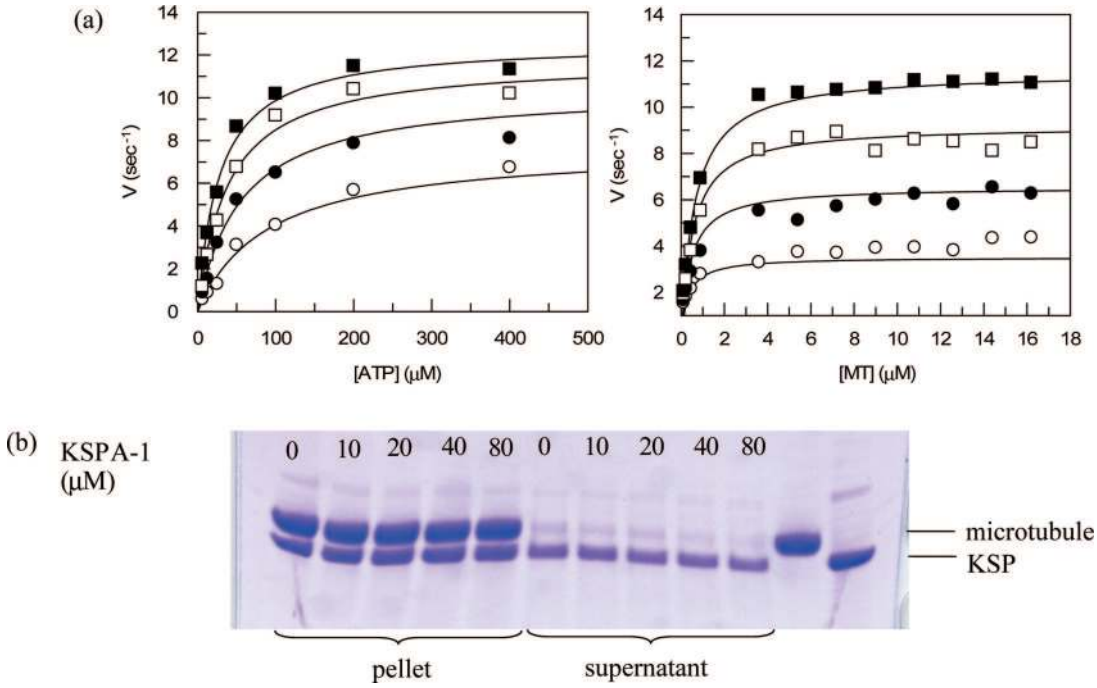

Figure 2. Mechanism of inhibition studies of KSPA-1. (a) Steady-state mode of inhibition studies by (left panel) varying the ATP concentration in the presence of saturating MT (9 μM) with 24 μM KSPA-1 (open circle), 8 μM KSPA-1 (filled circle), 2.7 μM KSPA-1 (open square), and 0 μM KSPA-1 (filled square); (right panel) varying the MT concentration in the presence of saturating ATP (200 μM) with 30 μM KSPA-1 (open circle), 10 μM KSPA-1 (filled circle), 3.3 μM KSPA-1 (open square), and 0 μM KSPA-1 (filled square). (b) Cosedimentation analysis of KSP binding to microtubules in the presence of varied concentrations (0 −80 μM) of KSPA-1.

In the presence of 50 μM KSPA-1, the k_{cat} of KSP basal ATP turnover increased 7-fold from 0.20 to 1.4 s^{-1}, while the K_m remained largely unchanged (Table 1), suggesting that the activation of basal KSP by KSPA-1 is mainly through an increased rate of catalysis (k_{cat} effect) but not better substrate binding (K_m effect). To understand better the mechanism by which KSPA-1 inhibits the MT-stimulated ATPase activity of KSP, we studied the mode of inhibition of KSPA-1 by steady-state kinetic analysis. The rate of MT-stimulated KSP-catalyzed ATP hydrolysis in the presence of varying concentrations of ATP and KSPA-1 were measured and the data were fit globally using the program Grafit (Figure 2a). Statistic testing (*F*-test) suggested that the data fit the best to a mixed-type mechanism with apparent $K_i = 6 \pm 1$ μM. Similarly, the rate of MT-stimulated KSP-catalyzed ATP hydrolysis in the presence of varying concentrations of MT and KSPA-1 were measured at saturating ATP concentration. The *F*-test results showed that KSPA-1 is clearly not competitive with respect to MT and the data fit best to a noncompetitive mechanism. In addition, KSPA-1 inhibits a KSP mutant with its loop L5 replaced by that of KHC (kinesin heavy chain, KHC-L5) with a $K_i = 1.2 \pm 0.3$ μM (see Supporting Information) and the inhibition here is also noncompetitive with respect to MT. This result contrasts with the effect of *Ispinesib* and other loop L5-binding inhibitors that display greatly attenuated affinity for the KHC-L5 relative to wild-type KSP, confirming that KSPA-1 inhibits KSP via a novel mechanism.[12]

Microtubule Binding Competition Assay. To further evaluate whether KSPA-1 directly competes with MT for KSP, an MT binding competition assay was performed. In this binding assay, 5 μM KSP and 5 μM MT were incubated with 0−80 μM KSPA-1 for 30 min at room temperature, then subjected to ultracentrifugation for 45 min and separated by SDS-PAGE. As shown in Figure 2b, the amount of KSP in the supernatant was not affected by increasing KSPA-1, confirming that the compound does not promote detachment of KSP from microtubules.

Effect of KSPA-1 on ADP Release. It is known that the rate-limiting step of basal KSP ATP hydrolysis is ADP release and that MT accelerates the KSP-catalyzed ATP hydrolysis reaction, mainly by accelerating the rate of ADP release.[10,21–23] Mant-ADP is a fluorescent ADP mimetic that can be conveniently used to spectroscopically follow the rate of nucleotide release from enzymes like KSP. We first tested whether Mant-ATP turnover could also be activated by KSPA-1. Using an assay detecting inorganic phosphate formation, both Mant-ATP and ATP reactions exhibited 8−9 fold activation by 50 μM KSPA-1, suggesting that the Mant-moiety of the nucleotide does not have an effect on KSPA-1 activation. KSPA-1 demonstrated a concentration-dependent acceleration of the rate of Mant-ADP release from KSP (see Figure 3 and Supporting Information). At a concentration of 80 μM, KSPA-1 accelerated the Mant-ADP release rate about 20-fold from 0.29 to 5.2 s^{-1} for MT-free KSP. In the presence of saturating MT, KSPA-1 has the opposite effect on Mant-ADP release from KSP, actually slowing the rate of nucleotide release by almost 3-fold (from 14.4 s^{-1} to 5.2 s^{-1}). These results clearly demonstrate that KSPA-1 augments basal ATPase activity by accelerating the rate-limiting ADP release step. Conversely, the compound inhibits MT-stimulated ATP turnover by decreasing the rate of ADP release to a rate similar to that of KSP in the absence of MT, presumably by diverting KSP to a nonproductive (or minimally productive) conformation.

(21) Cochran, J. C.; Sontag, C. A.; Maliga, Z.; Kapoor, T. M.; Correia, J. J.; Gilbert, S. P. *J. Biol. Chem.* **2004**, *279*, 38861–38870.
(22) Cochran, J. C.; Krzysiak, T. C.; Gilbert, S. P. *Biochemistry* **2006**, *45*, 12334–12344.
(23) Cochran, J. C.; Gilbert, S. P. *Biochemistry* **2005**, *44*, 16633–16648.

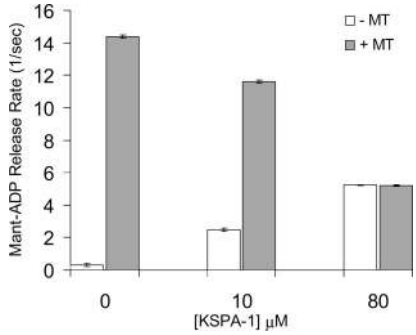

Figure 3. Mant-ADP release rate with and without MT in the presence of varied concentrations of KSPA-1.

KSPA-1 Inhibits Cell Proliferation by Inducing Monopolar-Spindle Formation. KSPA-1 inhibits the proliferation of HCT116 cells with an $IC_{50} = 28.1 \pm 0.8$ μM (Figure 4a). The mitotic activity of KSP is required for mitosis and its inhibition results in cell cycle arrest that is phenotypically characterized by the formation of monopolar spindles.[24] We investigated the mechanism of KSPA-1 cellular antiproliferative activity by evaluating the ability of the compound to induce monopolar spindles using immunofluorescence staining. As shown in Figure 4b, KSPA-1 induces monopolar spindle formation and this phenotype is indistinguishable from that seen with *Ispinesib* treatment of HCT116 cells. KSPA-1 compound showed no cytotoxicity up to 100 μM.

Hydrogen/Deuterium-Exchange (H/D-Ex) of KSP Motor Domain in the Presence of KSPA-1. Amide hydrogen/deuterium exchange (H/D-Ex), coupled with proteolysis and liquid chromatography−mass spectrometric analysis (LC−MS), is a very sensitive tool to probe protein conformation/dynamics.[18,25–27] Here, H/D-Ex was applied to measure the dynamics of KSP under four different conditions: in the presence or absence of ADP and in the presence and absence of KSPA-1 (summarized in Table 2 and Supporting Information 4). Under all conditions, 100% KSP sequence coverage was achieved in H/D-Ex experiments.

The H/D exchange pattern of a protein provides data on the dynamic properties of the protein in solution. Five segments 84−90 (helix α1), 95−99 (sheet β3), 157−160 (sheet β4), 257−263 (sheet β7), and 344−353 (helix α6) show less than 25% deuterium incorporation under all four tested conditions (Supporting Information 4). These segments, which are colored in blue in Figure 5a, are very close to each other in the X-ray crystallographic structure of KSP (PDB:1Q0B) and form the most stable core of this protein fold.[28]

In contrast, eight segments 4−21 (loop L1), 33−42 (β-turn), 54−69 (loop L2), 171−180 (loop L7), 214−227 (helix α3), 266−292 (loop L11), 305−316 (loop L12), and 354−368 (neck linker) show more than 75% deuterium incorporation under all four tested conditions (Supporting Information 4), indicating that these are very dynamic and solvent exposed regions (Figure 5b). As observed in many other proteins, the most dynamic and/or solvent exposed regions of the KSP motor domain are unstructured or loop regions. While segment 214−227 is part of helix α3 in the KSP-ADP structure, it is immediately adjacent to the switch I region of KSP. The switch I region, near the nucleotide-binding cleft, has been shown to dramatically alter its conformation, changing from a small helix or helices to a pseudo-β-hairpin in several other kinesin motor proteins.[29,30] It is thus conceivable that the part of helix α3 preceding switch I is structurally dynamic and could undergo conformational changes during the ATP hydrolysis cycle. As with most other kinesin motors, the structure of KSP motor protein resembles an arrowhead with the nucleotide binding site at the wider end

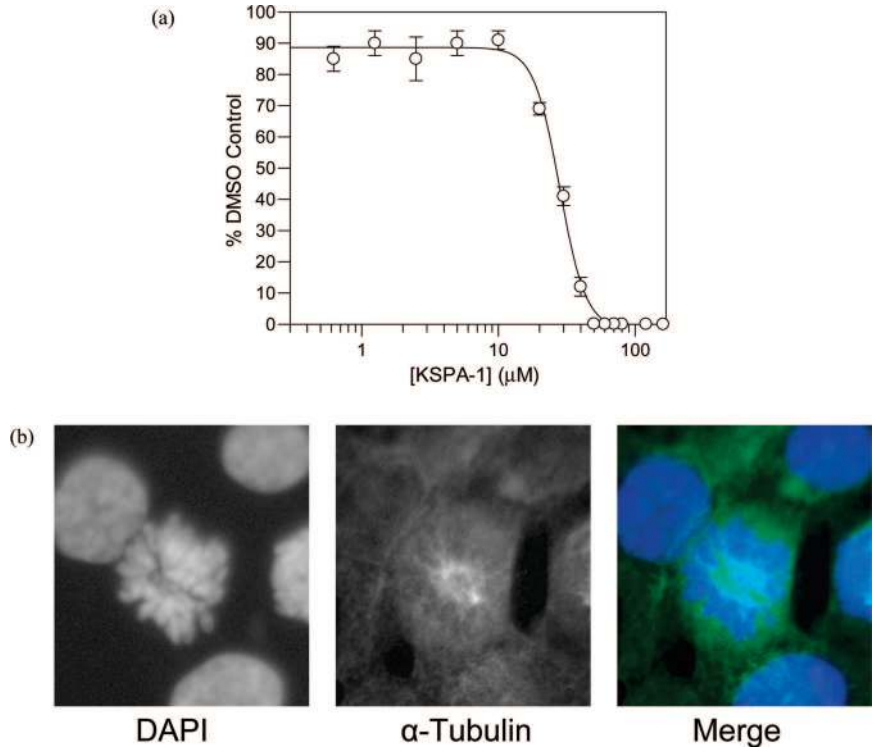

Figure 4. (a) Inhibition of HCT116 cell proliferation by KSPA-1. The IC_{50} value was determined by fitting inhibition data to the standard binding isotherm (eq 1). (b) KSPA-1 causes monopolar spindles in mitotic cells. Immunofluorescence staining [α-tubulin (green), chromatin (blue)] of HCT116 cells treated for 16 h with 0.4% DMSO (control) or 30 μM KSPA-1.

Table 2. Difference in Average Deuteration Level of Each Segment in KSP with and without KSPA-1 and/or ADP[a]

start[b]	end[b]	charge	(1) difference in H/D exchange 500 μM vs 0 μM ADP (%)	(2) difference in H/D exchange 600 μM vs 0 μM KSPA-1 (%)	(3) difference in H/D exchange 600 μM vs 0 μM KSPA-1 (500 μM ADP) (%)
4	21	2	0	2	−1
21	30	2	−2	1	−1
33	42	2	−4	3	1
40	51	2	−2	−1	1
54	69	2	1	2	1
72	81	1	−22	1	1
84	90	1	1	2	1
95	99	1	−7	2	2
105	124	2	−63	2	19
127	144	2	−37	1	0
147	154	2	3	−2	1
157	160	1	−3	1	2
163	168	1	−22	−4	1
171	180	1	−17	−3	1
187	201	2	−20	0	3
204	214	2	−13	1	2
214	227	2	−17	0	0
230	239	1	−9	0	−1
242	255	2	0	1	0
257	263	1	0	0	0
266	292	2	−7	0	2
295	301	1	−27	−6	18
305	316	2	−13	4	9
319	333	2	−19	1	5
336	343	1	−20	−3	0
344	353	0[c]	−10	−1	4
354	368	2	−7	−3	−3

[a] Column 1 shows the difference in average deuteration level with 500 μM ADP versus without ADP; column 2 shows the difference in average deuteration level with 600 μM KSPA-1 versus without KSPA-1 in the absence of ADP; column 3 shows the difference in average deuteration level with 600 μM KSPA-1 versus without KSPA-1 in the presence of 500 μM ADP. [b] The first two residues of each proteolytic fragment lose most of the deuterium attached during the separation step.[19] Therefore, peptide 2−21 can give the deuteration level of segment 4−21. This accounts for most of the gaps in the sequence. [c] The deuterium incorporation of segment 344−353 was obtained by the subtraction of the deuterium incorporation in 354−368 from that in 344−368.

of the arrowhead.[31] The deuterium incorporation results show that KSP motor protein has a rigid core consisting mostly of central β-sheets occupying the narrower end of the arrowhead (Figure 5). In contrast, the tail side of the arrowhead is more dynamic and may undergo conformational changes during the ATP hydrolysis cycle.

H/D exchange perturbations of KSP in the presence or absence of ADP were measured (Table 2). Overall, the protein has lower H/D exchange rates in most regions when ADP is present, suggesting that the KSP motor protein domain is less dynamic when ADP is bound. The segments that exchange significantly slower (>10%) in the presence of ADP are surrounding the three key regions for nucleotide sensing: the P-loop, switch I and switch II regions. Segment 105−124, the phosphate binding region (P-loop) of KSP, shows the most notable decrease (63%) in deuterium incorporation in the presence of ADP. The P-loop region is conserved in all kinesin structures and forms most of the nucleotide binding pocket. Almost all residues that have direct contact with ADP in the KSP structure are located within the P-loop region. In addition to the P-loop region, segments around the switch I and switch II regions also show significant decreases in H/D exchange rates (Figure 5b). The switch I and switch II regions are critical for nucleotide sensing and force production. These regions are proposed to consititute the main microtubule-binding elements of kinesins.[30,32,33] The decrease in H/D exchange in these regions upon ADP binding suggests that the presence of ADP allosterically reduces the dynamics of the switch II region.

In the absence of ADP, the binding of 600 μM KSPA-1 has very little effect on the H/D exchange rates of KSP with the only notable change being in segment 295−301 (helix α4) at the switch II region. The 6% decrease in H/D exchange in this segment indicates that this region is less solvent-accessible upon KSPA-1 binding. In the presence of 500 μM ADP, several regions of KSP show increases in deuterium incorporation with 600 μM KSPA-1 (Table 2). Three segments, 105−124 (P-loop), 295−301 (helix α4), and 305−316 (Loop L12), exchange significantly faster in the presence of 600 μM KSPA-1 (Figure 5c). Interestingly, these segments and their surrounding regions show significant reductions in H/D exchange when KSP binds to ADP (Table 2). Taken together, these observations suggest that the binding of KSPA-1 triggers conformational changes in the P-loop region and switch II cluster, accelerating the release of ADP.

Discussion

KSP is a promising new target for antimitotic cancer therapy. Its primary function in mitosis regulation and its absence in postmitotic neurons portend that inhibitors of KSP may block cancer cell proliferation without the neuropathic side effects typical of taxane and vinca alkaloid therapies.[1,3,14] Almost all of the small-molecule inhibitors of KSP known to date bind to an induced-fit pocket remote from the nucleotide binding pocket, providing exquisite selectivity for inhibitors targeting this site.[8,28] One exception is a marine natural product adociasulgate-2 (AS-2). AS-2 was identified as an MT-competitive inhibitor of conventional kinesin. It is a nonspecific kinesin inhibitor targeting mitotic and nonmitotic kinesins including KSP, CENP-E, RabK6, MKLP1, KHC, and KIFC1.[34,35] AS-2 forms rodlike aggregates with its sulfate groups exposed to aqueous solution and thus mimics MT in kinesin motor protein binding.[36]

In this study, we identified a novel class of compounds that can specifically inhibit KSP-MT complex catalyzed ATP

(24) Kapoor, T. M.; Mayer, T. U.; Coughlin, M. L.; Mitchison, T. J. *J. Cell Biol.* **2000**, *150*, 975–988.
(25) Busenlehner, L. S.; Armstrong, R. N. *Arch. Biochem. Biophys.* **2005**, *433*, 34–46.
(26) Chalmers, M. J.; Busby, S. A.; Pascal, B. D.; He, Y.; Hendrickson, C. L.; Marshall, A. G.; Griffin, P. R. *Anal. Chem.* **2006**, *78*, 1005–1014.
(27) Hamuro, Y.; Coales, S. J.; Morrow, J. A.; Molnar, K. S.; Tuske, S. J.; Southern, M. R.; Griffin, P. R. *Protein Sci.* **2006**, *15*, 1883–1892.
(28) Yan, Y.; Sardana, V.; Xu, B.; Homnick, C.; Halczenko, W.; Buser, C. A.; Schaber, M.; Hartman, G. D.; Huber, H. E.; Kuo, L. C. *J. Mol. Biol.* **2004**, *335*, 547–554.
(29) Marx, A.; Muller, J.; Mandelkow, E. *Adv. Protein Chem.* **2005**, *71*, 299–344.
(30) Kull, F. J.; Endow, S. A. *J. Cell Sci.* **2002**, *115*, 15–23.
(31) Turner, J.; Anderson, R.; Guo, J.; Beraud, C.; Fletterick, R.; Sakowicz, R. *J. Biol. Chem.* **2001**, *276*, 25496–25502.
(32) Nitta, R.; Kikkawa, M.; Okada, Y.; Hirokawa, N. *Science* **2004**, *305*, 678–683.
(33) Kikkawa, M.; Sablin, E. P.; Okada, Y.; Yajima, H.; Fletterick, R. J.; Hirokawa, N. *Nature* **2001**, *411*, 439–445.
(34) Brier, S.; Carletti, E.; DeBonis, S.; Hewat, E.; Lemaire, D.; Kozielski, F. *Biochemistry* **2006**, *45*, 15644–15653.
(35) Sakowicz, R.; Berdelis, M. S.; Ray, K.; Blackburn, C. L.; Hopmann, C.; Faulkner, D. J.; Goldstein, L. S. *Science* **1998**, *280*, 292–295.
(36) Reddie, K. G.; Roberts, D. R.; Dore, T. M. *J. Med. Chem.* **2006**, *49*, 4857–4860.

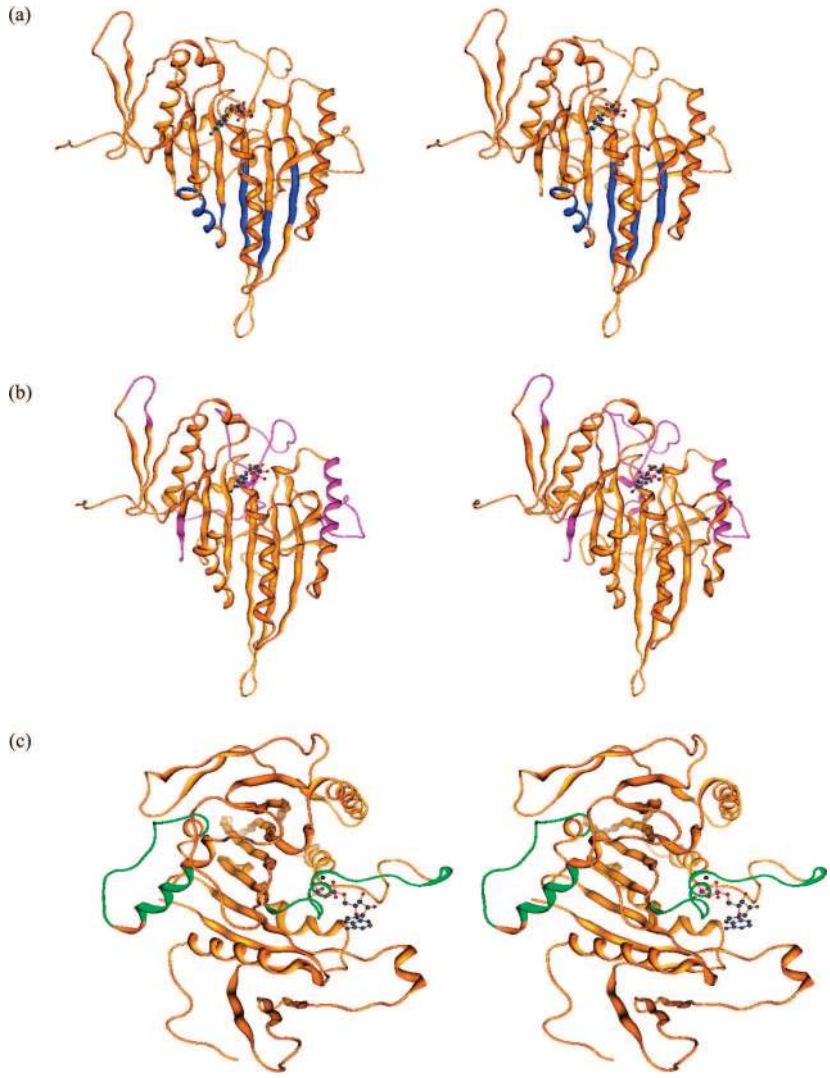

Figure 5. Stereoview of the modeled structure of KSP using the coordinates of crystal structure of KSP in complex with Mg-ADP (PDB: 1II6). The models are generated by projecting the average deuterium incorporation to KSP in the presence or absence of ADP or KSPA-1 onto the KSP crystal structure. (a) The segments with deuteration level <25% under all four different conditions are highlighted in blue and all the other segments are colored in orange. (b) The segments with deuteration level>75% under all four different conditions are colored in magenta and all the other segments are colored in orange. (c) The segments with significant change in deuterium incorporation (>9% change) in the presence of 600 μM KSPA-1 are highlighted in green and all the other segments are colored in orange. For all structures, the molecule at the active site of the KSP motor protein is ADP-Mg^{2+}.

hydrolysis. These compounds have differential effects on the KSP ATPase activities in the presence and absence of MT. KSPA-1, an exemplar of this class of compounds, accelerates the basal KSP-catalyzed ATPase reaction circa 10-fold while inhibiting the MT stimulated KSP-catalyzed ATPase activity with a $K_i = 6 \pm 1$ μM. KSPA-1 also inhibits the *Ispinesib*-resistant mutant KHC-L5 with a $K_i = 1.2 \pm 0.3$ μM, suggesting that KSPA-1 does not target the loop5 binding pocket. Unlike AS-2, KSPA-1 is very specific for KSP with no observable activation or inhibition effects on any other kinesins. In addition, KSPA-1 is noncompetitive with respect to MT and does not compete for MT binding in the MT binding assay. Single-turnover studies show that KSPA-1 augments the basal KSP-catalyzed ATPase activity by accelerating the rate-limiting ADP release step, similar to the mechanism of MT-stimulated ATP hydrolysis. It is unclear whether KSPA-1 and MT trigger the same "molecular switch" to accelerate ADP release.

To better understand the nature of KSPA-1 and KSP interaction, we used H/D exchange coupled with proteolyzis and mass spectrometry to study the solvent accessibility and protein dynamics for KSP. This approach has been successfully used to probe the interaction of KSP motor protein and several known inhibitors of KSP, including monastrol, *S*-trityl-L-cysteine, and AS-2.[34,37] We monitored the protein dynamics of KSP with and without ADP and KSPA-1. We observed that the nucleotide binding pocket and the loop regions are much more dynamic than the central β sheets and surrounding α helices (Figure 5a,b). Interestingly, ADP binding shows a dramatic effect on the solvent accessibility and protein dynamics of KSP (Figure 5c). Most regions have slower H/D exchange in the presence of ADP, with the most noticeable effect observed in the segments surrounding the key regions for nucleotide sensing: P-loop, switch I, and switch II regions. These results suggest that KSP is more rigid in the ADP-state compared to the nucleotide-free state. While binding of ADP drives the KSP into a rigid or "closed" state, binding of KSPA-1 has an opposite effect on the protein dynamics of ADP-bound KSP (column 3

(37) Brier, S.; Lemaire, D.; DeBonis, S.; Forest, E.; Kozielski, F. *Biochemistry* **2004**, *43*, 13072–13082.

of Table 2). In particular, the P-loop and the switch II helix α4 and loop L12 regions show significantly increased solvent accessibility upon binding to KSPA-1. These results, in conjunction with the results from kinetic analysis, suggest that KSPA-1 activates the basal KSP activity by driving the KSP protein from the "closed" ADP-state to a less rigid "open" state. An increase in deuterium incorporation in two regions was reported in a recent H/D Ex study of KSP in the presence of AS-2.[34] While the peptide 293−316 (helix α4 and loop L12) identified in the AS-2 study is almost identical to the region in which we observed significantly increased H/D-Ex (295−301 and 305−316 in Table 2), KSPA-1 binding induced no change in H/D-Ex in the other region, 161−189 (β4-L7-β5-L8-β5α). These results indicate that AS-2 and KSPA-1 both stimulate increases in dynamic motions of ADP-bound KSP, but are differentiated from one another by the specific details of the protein segments affected by each compound. Further structural studies are required to better understand the binding interaction between KSP motor protein and KSPA-1 and the mechanism of modulation.

KSP, like many other kinesins, uses the chemical energy of ATP hydrolysis to generate force and move along microtubules. The coupling of the chemical energy from ATP hydrolysis into mechanical movement is a complex process that involves conformational changes in different parts of the kinesin motor domain, offering multiple opportunities to intervene in this chemomechanical transduction pathway.[5,8–14] The "loop L5 binders" such as *Ispinesib* (SB715992), monastrol, *S*-trityl-L-cysteine, and dihydropyrazoles[5,8–14] block the KSP ATPase activity by locking the enzyme in a KSP-ADP-inhibitor ternary complex. AS-2, on the other hand, is a pan-kinesin inhibitor that mimics MT in kinesin motor protein binding and competes for MT binding. Recently, we reported a new family of ATP-competitive inhibitors of KSP that bind at the α4/α6 interface and likely interfere with the switch II−helix α4−helix α6−neck linker conformation relay.[38,39] KSPA-1, a representative of the maleamide KSP modulators, is a specific inhibitor of KSPATPase that inhibits the MT stimulated KSP ATPase acitivity but increases the basal KSP ATPase activity. KSPA-1 does not directly compete for MT binding and drives a conformational change in the KSP motor domain to disrupt the productive ATP turnover stimulated by MT. While previous reports have shown that the same small molecule could function as a receptor agonist or antagonist in the presence or absence of an auxiliary subunit,[40] KSPA-1 represents the first specific small molecule modulator that can activate an enzyme in one conformation while inhibiting it in another. These findings exemplify the diversity of novel mechanisms by which conformationally dynamic enzymes, such as KSP, can be targeted by small molecule effectors of catalytic function.

Acknowledgment. We thank William F. DeGrado and S. Walter Englander for helpful discussions regarding the use of hydrogen/deuterium-exchange analysis to characterize protein−ligand interactions.

Supporting Information Available: Complete author lists for refs 38 and 39. (1) Steady-state mode of inhibition study of KHL-L5 mutant; (2) presteady-state experiment for Mant-ADP release kinetics; (3) digestion/separation optimization of KSP; 4. KSP H/D-exchange results. This material is available free of charge via the Internet at http://pubs.acs.org.

JA710889H

(38) Parrish, C. A.; Adams, N. D.; Auger, K. R.; Burgess, J. L.; Carson, J. D.; Chaudhari, A. M.; Copeland, R. A.; Diamond, M. A.; Donatelli, C. A.; Duffy, K. J.; Faucette, L. F.; Finer, J. T.; Huffman, W. F.; Hugger, E. D.; Jackson, J. R.; et al. *J. Med. Chem.* **2007**, *50*, 4939–4952.

(39) Luo, L.; Parrish, C. A.; Nevins, N.; McNulty, D. E.; Chaudhari, A. M.; Carson, J. D.; Sudakin, V.; Shaw, A. N.; Lehr, R.; Zhao, H.; Sweitzer, S.; Lad, L.; Wood, K. W.; Sakowicz, R.; Annan, R. S.; et. al. *Nat. Chem. Biol.* **2007**, *3*, 722–726.

(40) Menuz, K.; Stroud, R. M.; Nicoll, R. A.; Hays, F. A. *Science* **2007**, *318*, 815–817.